



ELSEVIER

Available online at www.sciencedirect.com

SCIENCE @ DIRECT®

Global and Planetary Change 45 (2005) 249–263

GLOBAL AND PLANETARY
CHANGE

www.elsevier.com/locate/gloplacha

Spectral roughness of subglacial topography and implications for former ice-sheet dynamics in East Antarctica

Martin J. Siegert*, Justin Taylor, Antony J. Payne

Bristol Glaciology Centre, School of Geographical Sciences, University of Bristol, Bristol BS8 1SS, United Kingdom

Received 14 July 2003; accepted 28 September 2004

Abstract

Ice-sheet basal erosion is controlled by ice dynamics (including the basal thermal regime) and the lithology of the substrate. Spatial variation in subglacial roughness is therefore likely to be a function of these controls. In Antarctica, very little is known about former ice dynamics and sub-ice geology. Here, we calculate the spectral roughness of subglacial East Antarctica from an analysis of radio-echo sounding data. As the modern glaciological setting is understood reasonably well in East Antarctica from numerical ice-sheet modelling, we are able to compare the roughness calculations with contemporary ice-sheet dynamics. We show that ice divides at Ridge B and Dome A are underlain by rough terrain and a cold thermal regime. At the Dome C ice divide, however, the bed is noticeably smooth at the shorter wavelengths (~5–10 km) but rougher at longer wavelengths. One interpretation is that subglacial morphology has been eroded, leaving a smoothed landscape that contains valleys and hills. Regardless of the origin of the valleys, their erosion is only possible if the ice sheet were more dynamic than at present. Hence, whereas Dome A and Ridge B have a bed morphology consistent with the present ice sheet, the morphology at Dome C is likely to predate the present ice-sheet configuration.

© 2004 Elsevier B.V. All rights reserved.

Keywords: East Antarctica; Subglacial topography; Ice-sheet dynamics

1. Introduction

Radio-echo sounding (RES) has been used to measure the subglacial morphology of ice sheets for over 30 years (e.g., Robin, 1969). Maps of bed relief have been constructed for Greenland and Antarctica

using RES measurements as input to interpolation models (Drewry, 1983; Lythe et al., 2001; Bamber et al., 2004). Although interpolations vary in sophistication, the procedure essentially adds values where no data have been taken and smoothes the topography where measurements have been acquired to build a 'gridded' data set (Drewry, 1983; Lythe et al., 2001). This makes an assessment of sub-ice topographic roughness (i.e., the wavelength-related undulation of a surface) from bed maps problematic. Roughness

* Corresponding author. Tel./fax: +44 117 928 8902.

E-mail address: m.j.siegert@bristol.ac.uk (M.J. Siegert).

calculations can be made, however, along the track of RES flightlines because the data are continuous and uninterpolated.

Subglacial roughness is dependent on four factors: (1) the direction of ice flow, since the bed may be smoother along the direction of ice flow and rougher orthogonal to ice flow; (2) ice dynamics, as warm ice that is sliding will cause more erosion than ice frozen to the bed; (3) lithology, because soft beds will erode more easily than hard beds will; and (4) geological structure, as the roughness of a surface can be related to existing bedding, folds, and faults. These factors could be subject to change over time scales on the order of a few million years. Change to ice flow and dynamics has been advocated in East Antarctica by several groups, although others propose stable conditions over the last few million years (Miller and Mabin, 1998). Lithological change at the ice-sheet base is possible under a scenario involving the erosion and deposition of sediment. It should be noted, however, that the geology of East Antarctica is poorly constrained. The analysis of nunataks and outcrops at the ice-sheet margin reveals the East Antarctic craton to have been developed from the breakup of Gondwanaland during the Mesozoic Era (Dalziel and Lawver, 2001). There is, however, no direct sample of material from under the ice sheet, which makes it impossible to establish a detailed geological setting for East Antarctica.

Here, we detail the roughness of subglacial East Antarctica from the spectral analysis of RES data. Roughness calculations are compared with numerical ice-sheet modelling results to establish relationships between modern ice-sheet dynamics and the roughness of its bed, which are then used to infer associations between spatial variations in roughness, lithologies, and former ice-sheet dynamics. Ice-sheet modelling is also used to identify previous ice-sheet configurations that may account for discrepancies between the modern ice-sheet thermal regime and subglacial roughness. In particular, we aim to identify whether the roughness of subglacial East Antarctica is consistent with an unchanging or changeable ice mass.

We note that there is a causality issue regarding bed roughness and ice dynamics. Roughness controls ice flow because soft, smooth topographies are likely to reduce basal friction and promote fast flow. Conversely, flow controls roughness through subglacial

erosion. Regardless of which is dominant, we contend that there must be an association between bed morphology and ice dynamics, and this contention is the basis of our investigation.

2. Radio-echo sounding data

The most extensive RES survey of East Antarctica (by area of coverage) was undertaken between 1971 and 1979 by the Scott Polar Research Institute (SPRI), University of Cambridge (Drewry, 1983). In this survey, over 200,000 km of flight track were acquired across approximately 40% of the ice sheet. The region between Ridge B and Dome C was surveyed particularly well, and a less dense network of flights was also made between Ridge B and Dome A, and around the South Pole (Fig. 1). Bedrock returns were obtained along the majority of tracks. Time-continuous recordings of echo soundings were assembled as the ‘Z-scope’ output (Fig. 2) and digitised at 20-s time-interval markers from the Z-scope record. This results in a data point ground-spacing of approximately 1.6 km (1 mile).

The survey was organised as a series of orthogonal flightlines separated by between 50 and 100 km. Hence, a series of bedrock profiles, in both electronic file and Z-scope format, was recorded in two directions across a large proportion of the East Antarctic Ice Sheet.

These RES data have been used previously to identify and locate subglacial lakes (Siegert et al., 1996; Dowdeswell and Siegert, 1999) and regions of potential water-saturated basal sediments (Siegert and Ridley, 1998; Siegert, 2000) from the bright, flat specular returns that are expected to occur over basal water bodies. In none of these investigations was the spectral roughness of basal topography examined.

3. Calculating basal roughness

The RES data used here are unmigrated. The effect of high relief or discontinuities in the bed is to produce diffractions. Similarly, steep slopes generate offsets in the plotted position of the reflectors. The overall outcome of both effects is to smooth out relief (Kearey and Brooks, 1991). Consequently, bed roughness

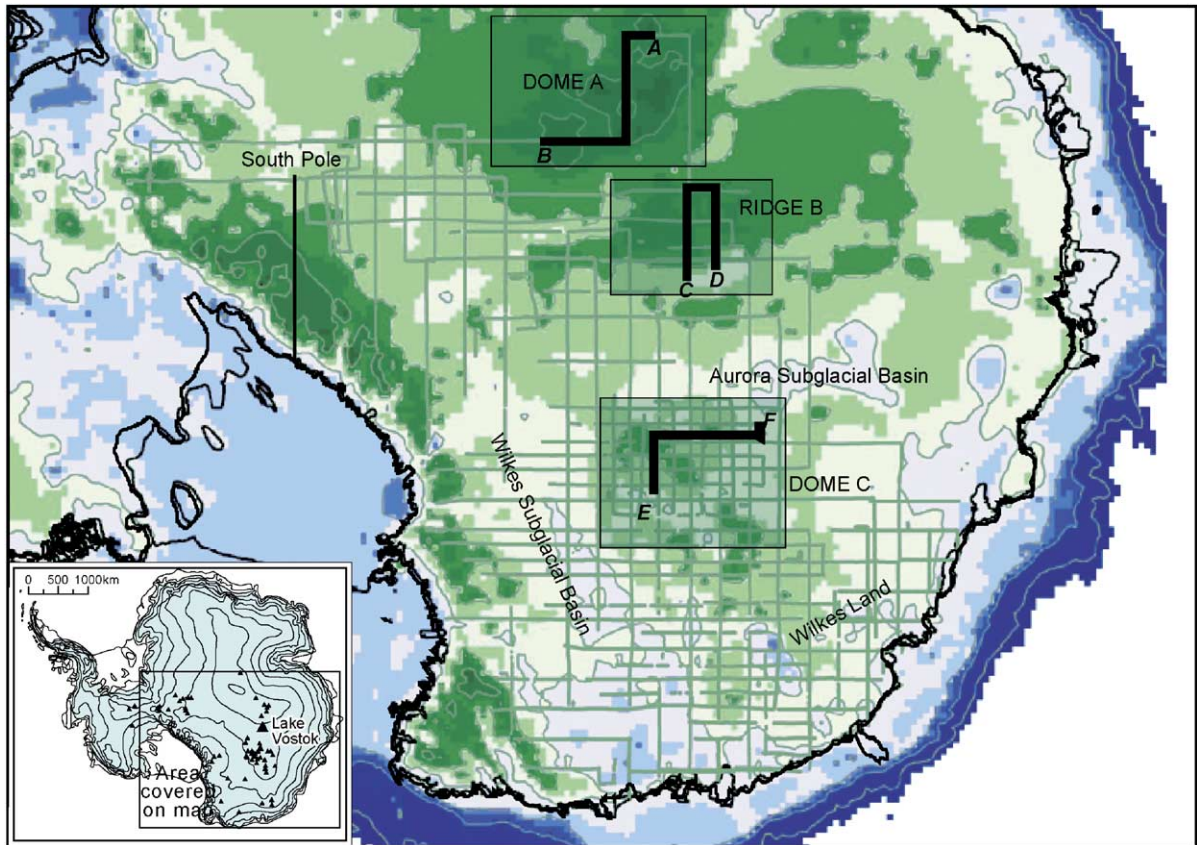


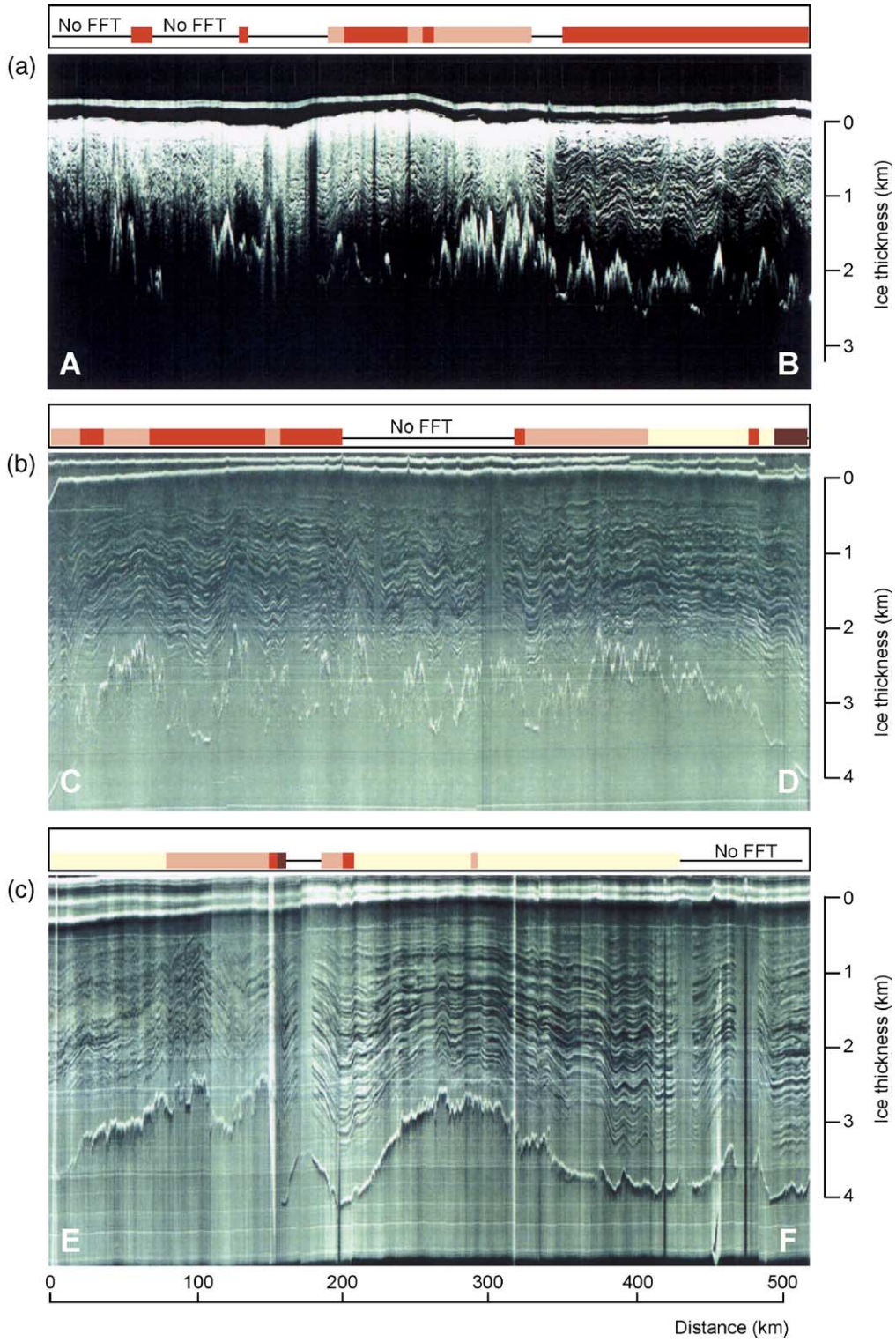
Fig. 1. Relaxed bed topography of East Antarctica under the cover of the SPRI RES survey. The topography was calculated by accounting for the isostatic uplift that would occur under the complete deglaciation of the continent, using the modern bed and ice thickness data, as depicted in the BEDMAP database (Lythe et al., 2001), and sea level 120 m higher than at present. Contours are provided every 500 m, and the sea-level contour separates blue and green shaded regions. The SPRI RES flightlines used in this paper are superimposed, and the locations of transects AB, CD, and EF (presented in Fig. 2) are provided. Shaded areas refer to zones where total roughness power spectra were calculated (presented in Fig. 4). The inset shows the location of the study region and the distribution of subglacial lakes (\blacktriangle ; Siegert et al., 1996).

calculations are minimum values, and we expect the relative spatial variation in roughness to be unaffected. Roughness power spectra were calculated following Taylor et al. (2004), over a moving ~ 100 -km window along each flight line. This results in a number of data gaps where the bed echo is lost due either to the absorption of the radio wave or turning of the aircraft (i.e., a corner of a flight line).

Power spectra were calculated using the forward Fast Fourier Transform (FFT) capabilities in the Microcal Origin 5.0 software (a discrete Fourier transform). Preconditions for the calculation are the use of 2^N data points. In practice, this limits the minimum length of the RES line for a single bed roughness power spectra to 80–110 km, depending on

the along-track resolution ($N=5$). Lines of less than this length were ignored. Each ~ 100 -km window is then detrended using least-squares regression, to remove the dominance of very long wavelength roughness. Amplitude is normalised with respect to N , following Hubbard et al. (2000). The resulting power spectra are dimensionless in the y (vertical) direction. Frequency f (x , horizontal coordinate) is then converted to wavelength λ (km).

The scales of the bed roughness identified are limited by the along-track resolution of the bed data set. The following scales of bed roughness (being the integral part of the FFT power across the relevant part of the frequency domain) are used: long (>20 km), medium (10–20 km), and short wavelengths (~ 5 –10



km). We note that the short-wavelength component cannot be used to distinguish the presence or absence of individual geomorphological landforms because, in the data available, the along-track sampling resolution is too small (e.g., Ó Cofaigh et al., 2002).

4. Spatial variations in basal roughness

The base of the East Antarctic Ice Sheet is organised into coherent geographic areas, which have specific roughness characteristics (Fig. 3). We define three bed roughness groups (see Table 1). Regions within Group 1 are rough at all scales: Dome A, Ridge B, and an area west of, and including, the Porpoise Subglacial Highlands across Wilkes Land. Group 2 comprises the area around Dome C, which is mostly smooth at short wavelength but rougher at medium and long wavelengths. Group 3 consists of the Wilkes Subglacial Basin and the Aurora Subglacial Basin (between Dome C and Ridge B, including the Lake Vostok locale), which are smooth at all measured wavelengths. Group-3-type roughness values have previously been established across the Siple Coast region of West Antarctica, where a soft sedimentary substrate is thought to exist (Siegert et al., 2004). At long wavelengths, these three locations have a roughness similar to that over the majority of Dome C (Group 2).

Fig. 4 shows the full power spectra for the bed at Dome A, Ridge B, and Dome C ice divides in the two flight directions (within areas denoted in Fig. 1). The bed beneath Dome A appears roughest of the three ice divides (Fig. 4a). Here, the bed roughness spectra show noticeable power levels across most wavelengths. Ridge B is only slightly smoother (Fig. 4b). The flight lines across Ridge B are located parallel and orthogonal to the ice flow. Here, there is only limited evidence (from roughness calculated with a 3.5-km interval) that the power spectra differ in relation to flight orientation and, hence, ice flow direction (Fig. 4b). At Dome C, the power levels of bed roughness are noticeably lower at all wavelengths than at Ridge B and Dome A (Fig. 4c). In fact, at high wavelengths, there is hardly any

measurable roughness across the bulk of the Dome C region (Fig. 4). The exception to this is across the central part of Dome C (see ~100–150 km in Fig. 2c), where the roughness is greater.

There is little correlation between bed elevation and roughness at the medium and long scales (Fig. 3). However, roughness at short wavelength is generally low when the bed is below sea level and is roughest at bed elevations between 0 and 1000 m a.s.l. (Fig. 3a). In addition, there appears to be no relation between ice thickness and bed roughness.

To interpret the patterns of bed roughness in East Antarctica, an appreciation of the modern glaciological setting is required. The macrodynamics of the Antarctic Ice Sheet can be identified from ice surface and thickness maps (e.g., Drewry, 1983; Lythe et al., 2001) and from numerical ice-sheet modelling, which provides information on basal ice dynamics and subglacial thermal conditions.

5. Numerical ice-sheet modelling

Direct measurement of the basal thermal regime of the East Antarctic Ice Sheet is not possible. We therefore resort to the use of a numerical model of ice flow and temperature evolution. The model is similar to one used in previous studies of the West Antarctic Ice Sheet (Payne, 1998, 1999). It simulates the coupled evolution of ice velocity, thickness, and temperature, as well as the isostatic response of the underlying bedrock. The physics incorporated within this type of model is now fairly standard (with the exceptions noted below). Ice thickness evolves as a function of the local snow accumulation and the horizontal flow convergence and divergence within the ice mass. Ice flow is determined by assuming a simple stress balance, in which gravitational driving stresses are balanced locally at the bed, and assuming that ice deforms according to Glen's Flow Law (which is corrected for the effects of ice temperature on its viscosity). The evolution of the internal distribution of temperature is determined by considering processes such as diffusion, advection

Fig. 2. Raw RES data from three transects (a) AB, across Dome A, (b) CD over Ridge B, and (c) EF along Dome C. The position of each transect is provided in Fig. 1. Along-track bed roughness at all frequencies (i.e., the total power derived from a power spectrum, Fig. 4) is provided above each transect in the same format as that given in Fig. 3 (darker pinks describing rougher bed).

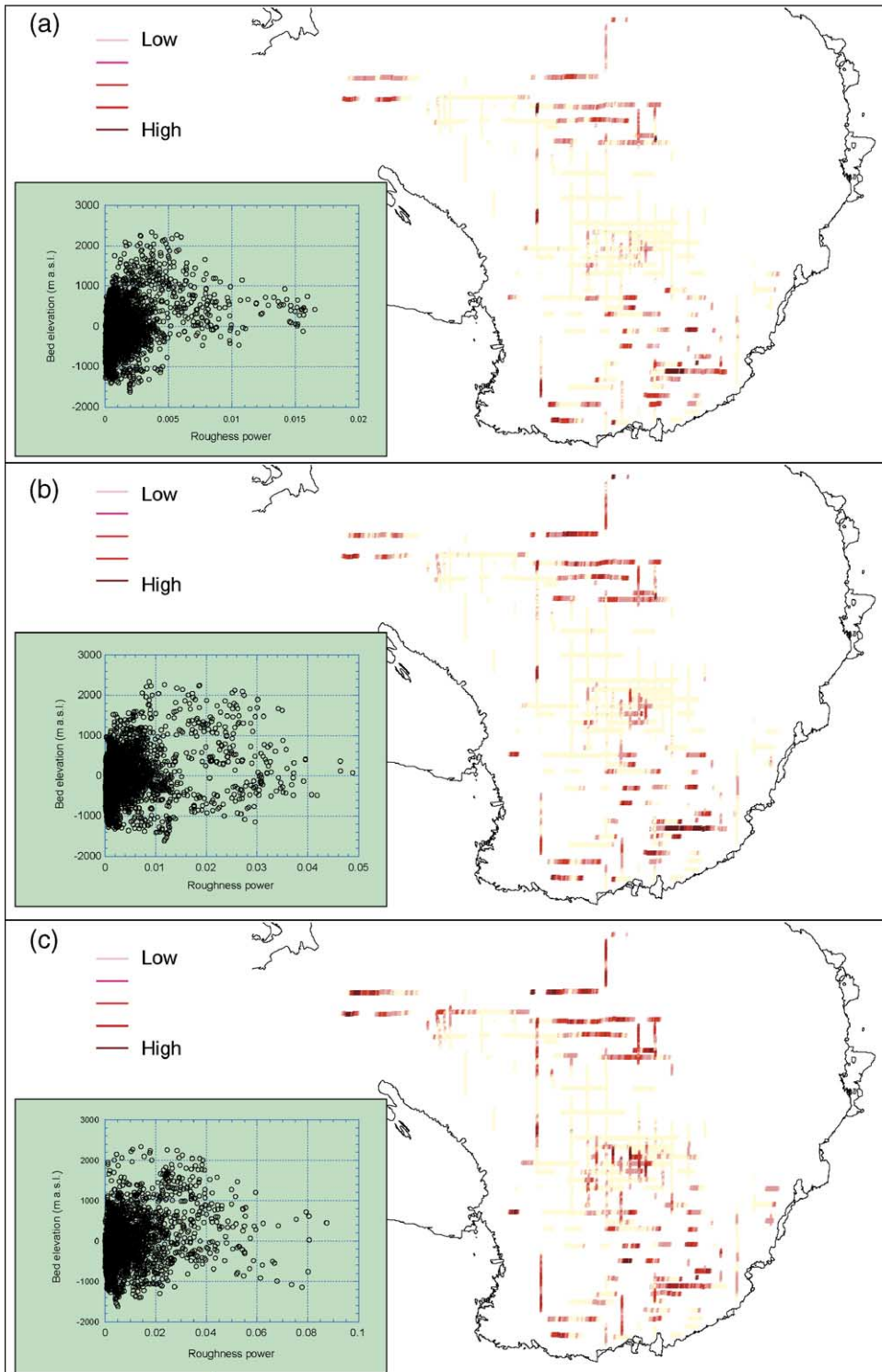


Table 1

Summary of subglacial roughness (as measured by RES) and the modern ice-sheet thermal regime and dynamics (as described by a numerical thermodynamic ice-sheet model)

Locale	Bed roughness	Group	Presence of water	Presence of sliding	Implications
Dome A	High at all measured wavelengths Fig. 2a	1	N	N	Subglacial roughness is consistent with modern ice sheet.
Ridge B	High at all measured wavelengths Fig. 2b	1	N	N	
Dome C	Mostly low only at shortest wavelength (~5–10 km), high at all others Fig. 2c . Subglacial troughs preserved within a smoothed landscape.	2	Y	N	Subglacial roughness appears inconsistent with modern ice sheet. Morphology may thus predate the current ice sheet form.
Porpoise highlands	High at all measured wavelengths.	1	N	N	Subglacial roughness is consistent with modern ice sheet.
Aurora basin	Low at all measured wavelengths. Relief is generally low and landscape is smooth.	3	Y	Y	Subglacial roughness is consistent with modern ice sheet and with an ice sheet whose margin migrates across these regions.
Wilkes basin	Low at all measured wavelengths. Relief is generally low and landscape is smooth.	3	Y	Y	Subglacial sediments may exist across much of these regions (e.g., Siegert, 2000).

(both horizontal and vertical), and heat generation by internal dissipation and friction at the bed. The equations representing these processes are solved using the finite-difference technique on a regular spatial grid of resolution 20 km and the vertical coordinate system that is conformal to local ice thickness.

The model is primarily used to understand the present-day configuration of the East Antarctic Ice Sheet. The principal inputs to the model are present-day air temperature and snow accumulation patterns ([Giovinetto et al., 1990](#) and [Vaughan et al., 1999](#), respectively) and bedrock topography (the recent BEDMAP compilation is employed, [Lythe et al., 2001](#)), as well as geothermal heat flux. This latter quantity is very poorly defined, and we choose a spatially uniform value of 60 mW m^{-2} . This value generates a reasonable fit to the temperature profiles

obtained from a range of deep ice cores such as Vostok, Byrd, and Siple Dome. We have performed a sensitivity analysis around this value and find that the interpretations presented here are robust, within the range 50 to 70 mW m^{-2} . It is unlikely that the real values of geothermal heat flux fall outside this range ([Siegert and Dowdeswell, 1996](#)).

The model is allowed to run until a steady-state thermal regime develops. This typically takes 100,000 years. During this time, the extent of the grounded ice sheet is held constant to within its present-day grounding line. This approach simplifies the design of our numerical experiments and is unlikely to affect the predicted thermal regime, except in areas very close to the grounding line (which, in reality, may still be responding to grounding lines changes associated with the Last Glacial Maximum). The model predicts considerable time-dependent behaviour associated

Fig. 3. Along-track roughness of subglacial topography at three frequency bands: (a) high frequency (bed wavelengths ~5–10 km), (b) medium frequency (bed wavelengths between 10 and 20 km), and (c) low frequency (bed wavelengths >20 km). The relationships between roughness and bed elevation for each frequency are provided in the insets. [Fig. 2](#) shows how the along-track roughness colour scheme relates to actual RES data.

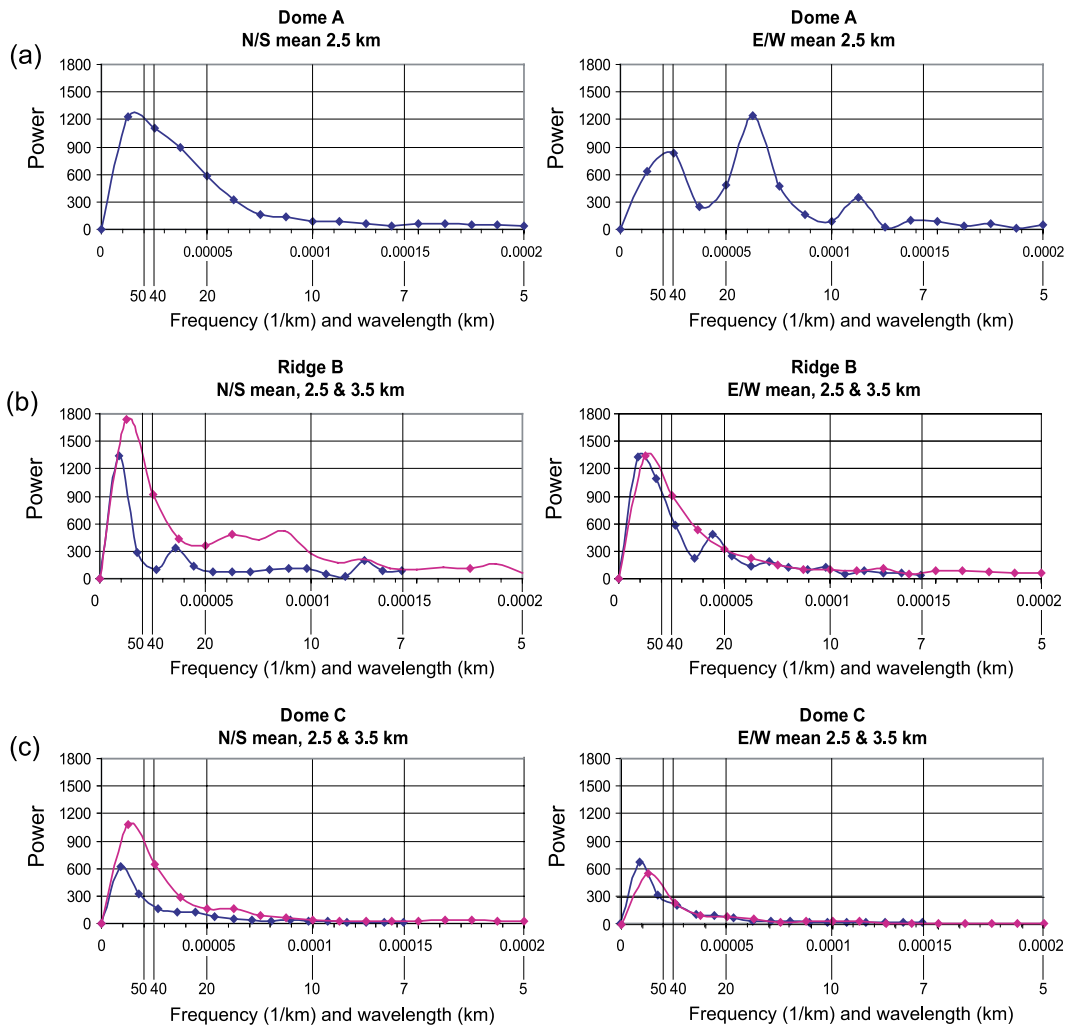


Fig. 4. Power spectra for three regions of East Antarctica: (a) Dome A, (b) Ridge B, and (c) Dome C (the locations of which are provided as shaded regions in Fig. 1). For each region, power spectra are provided in two directions, relating to the orientations of the flightlines. Furthermore, for Ridge B and Dome C, roughness powers are given using data with a spatial interval of 2.5 (blue) and 3.5 km (pink), whereas at Dome A data have a space interval of 2.5 km.

with the stagnation and lateral migration of ice streams. The results we present here have therefore been averaged over the final 1000 years of the model run.

A simple model of the ice sheet's basal hydrological regime is incorporated. A local budget is determined for water depth at each grid point (W) as follows:

$$\frac{dW}{dt} = M - \frac{W}{\lambda},$$

where M is the basal melt rate, and the time constant (λ) is set to 20 years on the basis of observed water flow

rates (based on observations by Engelhardt and Kamb, 1997).

Fig. 5 shows the predicted basal thermal regime and water depths. The patterns in both fields are generated by a combination of bedrock topography and ice flow. Bedrock troughs tend to be associated with warmer ice because of the enhanced thermal insulation afforded by thicker ice as well as heat generation by fast ice flow. The same processes operating in reverse lead to bedrock massifs being associated with cooler basal temperatures (e.g., the

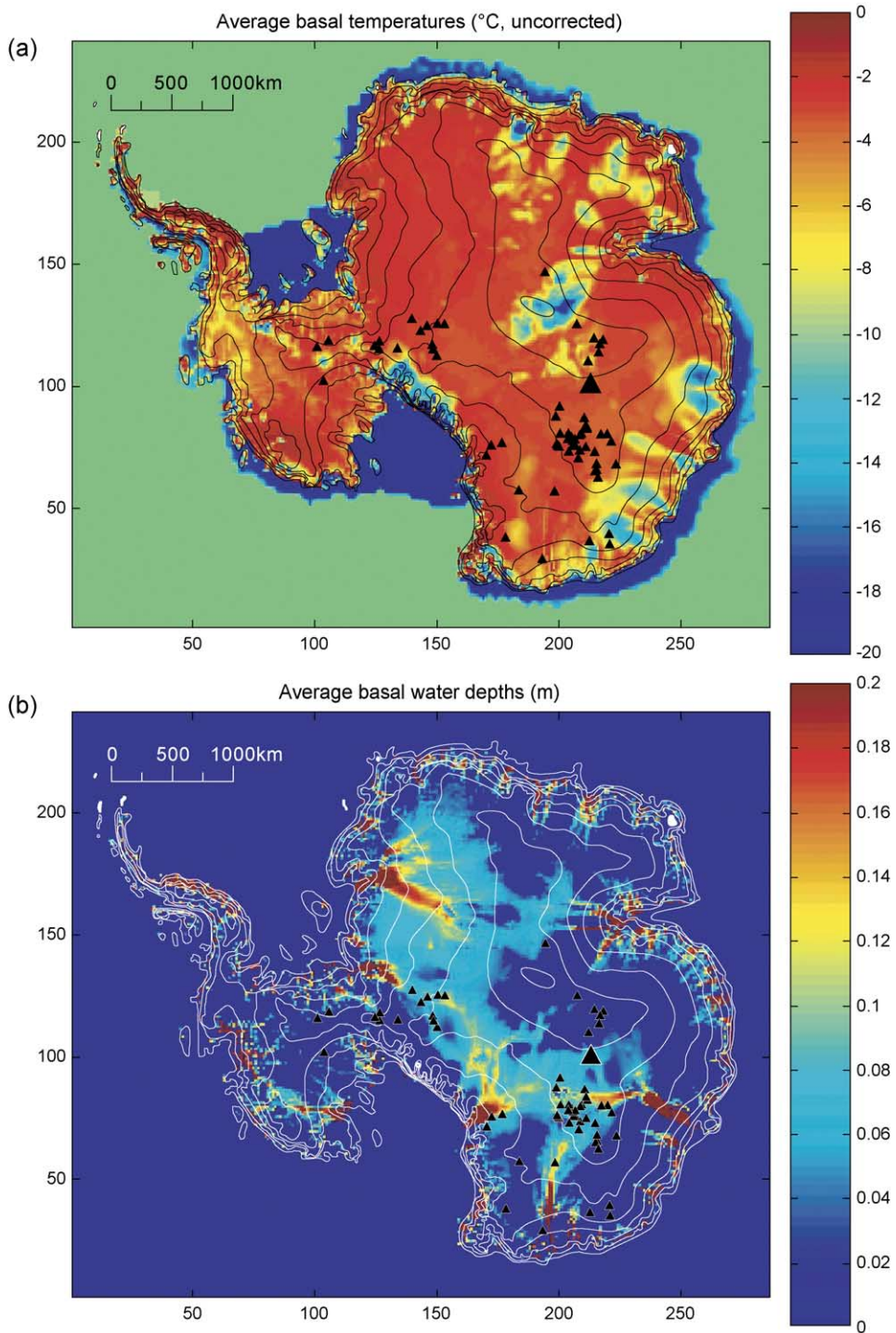


Fig. 5. Numerical ice-sheet modelling of the present ice sheet: (a) subglacial temperatures ($^{\circ}\text{C}$) and (b) basal water depths (m). Ice surface contours are provided (500-m intervals), as are the locations of subglacial lakes (given as triangles, Lake Vostok is the largest triangle).

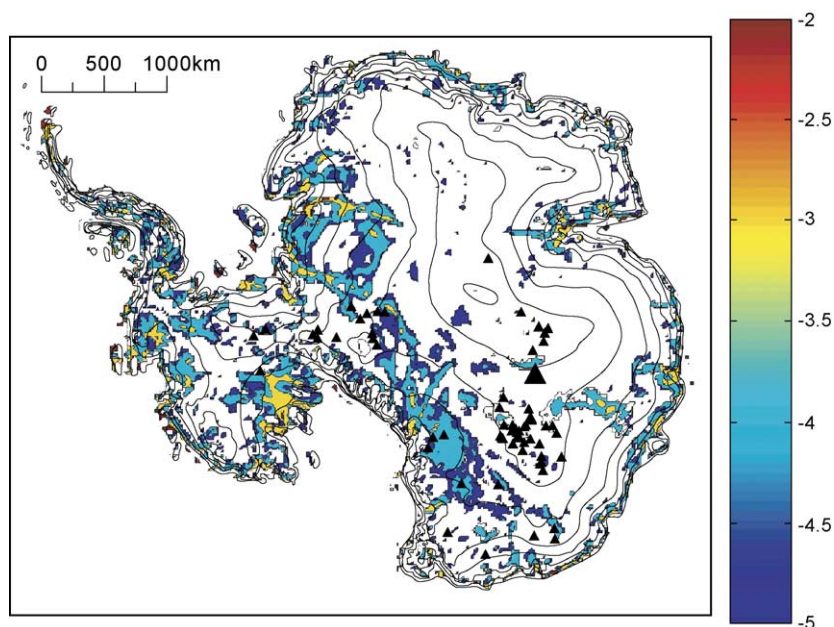


Fig. 6. Subglacial slip coefficients, calculated as the difference between balance velocities and velocity due to the deformation of ice, divided by the gravitational driving stress (in $\text{m yr}^{-1} \text{Pa}^{-1}$). Ice surface contours are provided (500-m intervals), as are the locations of subglacial lakes (given as triangles, Lake Vostok is the largest triangle). The white zones denote where zero slip is predicted.

Gamburtsev Subglacial Mountains at Dome A). The strong control of bedrock topography on the thermal regime implies that the model predictions must be treated with caution in areas where the bedrock topography is poorly constrained by RES observations in the BEDMAP data set (see Lythe et al., 2001, for details). The patterns shown in Fig. 5 are compared with the location of known subglacial lakes (Siegert et al., 1996) under the assumption that subglacial lakes should only occur where the model predicts basal melt. The model performs reasonably well in this respect; however, the cluster of lakes around the Lake Vostok-Ridge B area is not associated with predicted basal melt. This may be due to inadequacies in the BEDMAP database, which interpolates across RES flightlines (often separated by 50 km) and, in doing so, smooths the bed profile. In particular, the bedrock topography in the area around Lake Vostok is poorly constrained by RES observations within the BEDMAP database.

In the model, basal slip is assumed to be proportional to gravitational driving stress, with the constant of proportionality (B) a function of water depth (a tanh function is used). This parameterization

was calibrated by comparing ice fluxes determined on the basis of mass continuity (by integrating snow accumulation upstream of a location) minus the contribution of ice deformation, with gravitational driving stress. The results of this analysis are shown in Fig. 6.

6. Glaciological setting and bed roughness

Below, the modern subglacial thermal regime and dynamics are described for each of the three groups of subglacial roughness, and a summary is presented in Table 1.

6.1. Group 1: Ice divides at Dome A and Ridge B

Ice divides at Ridge B and Dome A are likely to be frozen at the ice-sheet base. At Dome A, basal temperatures are calculated to be as low as $-20\text{ }^{\circ}\text{C}$, while at Ridge B, the basal temperatures are around $-10\text{ }^{\circ}\text{C}$ (Fig. 5). It is unlikely that basal temperatures here would have been significantly different from these values over a glacial–interglacial cycle, as the

ice thickness in central East Antarctica changes by only a few hundred metres (e.g., Huybrechts, 2002). The areas of frozen basal ice correspond with the location of rough topography (Figs. 3 and 5). Hence, we expect the ice divides and Ridge B and Dome A to be frozen to their base for as long as the ice sheet has been at its present continental scale, and we link these long-term conditions to the development or preservation of rough subglacial terrain.

6.2. Group 1: Porpoise Subglacial Highlands (and Wilkes Land)

West from the Porpoise Subglacial Highlands, across Wilkes Land, the bed is rough at all scales (similar to Dome A). The ice sheet here is cold based. In fact, the basal temperatures are extremely low (around -15°C), suggesting that the ice sheet is unlikely to have been warm based here in the past.

6.3. Group 2: Dome C ice divide

At Dome C, the ice is likely to be warm based and a source for significant water generation (Fig. 5). Modelling the basal slip coefficient shows, however, that there is virtually no subglacial sliding at Dome C (Fig. 6). The current ice-sheet configuration is thus not conducive to erosion, hence, bedrock smoothing in this area is unlikely. The bed across the majority of Dome C is smooth at high frequencies and rough at the medium and long wavelengths, which correspond to large-scale morphological features, such as valleys and overdeepened troughs. We assume the bed has been rougher at some stage in the past, since the small area around the central, highest part of Dome C (see 100–150 km in Fig. 2c) is noticeably rougher than the adjacent surrounding bed. The formation of this landscape is unlikely to have occurred under the present ice sheet.

6.4. Group 3: Wilkes and Aurora subglacial basins

The Wilkes Subglacial Basin is characterised by warm subglacial temperatures (i.e., basal ice at the pressure melting point), the production of subglacial water and basal sliding across much of its area, and extremely smooth bedrock (Figs. 3, 5, and 6). These characteristics seem highly compatible. The roughness

of the bed is similar to that beneath the Siple Coast ice streams (Taylor et al., 2004), and hence, the bed of the Wilkes subglacial basin could consist of water-saturated sediments. The elevation of the bed is currently below the sea level, but in a relaxed (ice-free) state, most of the region would be subaerial (Fig. 1).

The bed across the Aurora Subglacial Basin is smooth at all scales. Ice-sheet modelling indicates that the bed is water saturated here and that there is considerable production of meltwater (Fig. 5). Furthermore, basal sliding is predicted, albeit at a level reduced from that expected across the Wilkes Subglacial Basin (Fig. 6).

7. Implications for former ice-sheet dynamics and subglacial geology

7.1. Evidence in support of stable ice-sheet conditions

The subglacial bed that is rough at all scales is predicted to be overlain by cold-based ice. In most cases, the ice is several degrees below the pressure melting point, indicating that it is unlikely that it was warm based in the past. Where the ice sheet is smooth at all frequencies, on the other hand, basal temperatures are warm, there is considerable production of meltwater, and basal sliding is predicted. The ice-sheet dynamics therefore seem to be compatible with the basal roughness characteristics, and from this, one could argue that the present ice-sheet configuration and subglacial roughness are mutually compatible. If so, this arrangement would support the argument for a stable East Antarctic Ice Sheet for the past 15 million years or so (Miller and Mabin, 1998).

7.2. Evidence in support of previous ice-sheet variation

At Dome C, however, basal roughness is smooth at high frequencies and rough at low frequencies. This indicates that subglacial erosion has occurred to some degree and that large-scale morphological features, such as troughs and valleys, of which there are several examples, dominate the relief. The origin of these landforms is contentious. One possibility is that they are rift valleys. An alternative possibility is that they are glacially formed troughs (Drewry, 1975). Such a

genesis requires the ice sheet at Dome C to be both more dynamic than at present and flowing radially from the centre of Dome C (where roughness is greatest).

At Dome C, Rémy and Tabacco (2000) identified small-scale streamline bed forms, trending south–north, which they interpreted as tectonic pre-ice-sheet landforms. An alternative explanation is that the streamlined bed morphology at Dome C was formed subglacially by an ice sheet that had a noticeable surface gradient across what is now the Dome C ice divide.

7.3. Evidence for geological variations in East Antarctica

A further explanation for the bed roughness contrasts in East Antarctic is that they are caused by geology. For example, the smooth topography across the Wilkes and Aurora subglacial basins could be due

to the presence of un lithified sediments, whereas over Ridge B, Dome A, and the Porpoise subglacial highlands, hard erosion-resistant rock is compatible with the high roughness measurements. Although it is appropriate to mention the possible connection between roughness and lithological variations, in the absence of rock samples from the ice-sheet base, it is not possible to develop this connection. Future ice coring at Dome C by the EPICA consortium will retrieve a bedrock sample. It may therefore be possible to further understand the link between past ice-sheet dynamics, geology, and subglacial roughness subsequent to current ice coring activities.

8. Testing the likelihood of former dynamic behaviour at Dome C

Numerical ice-sheet modelling is used to examine the conditions that would permit dynamic ice

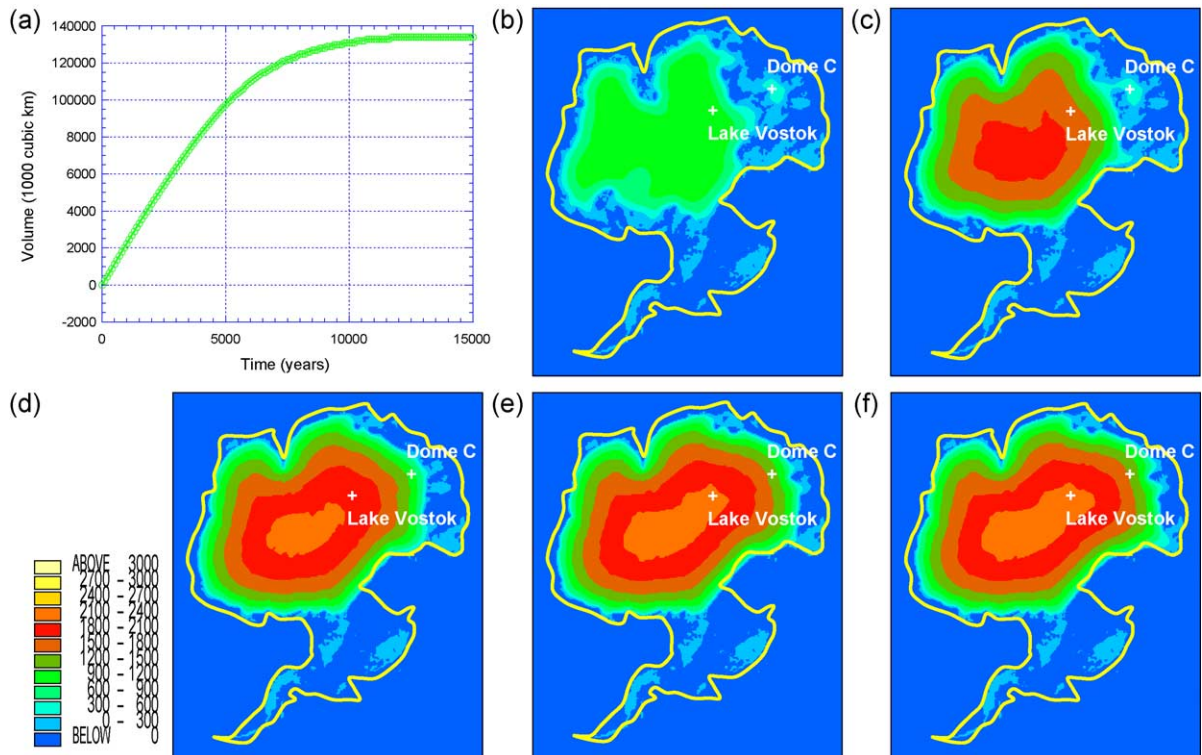


Fig. 7. Numerical ice-sheet modelling results of ice growth in East Antarctica, starting from zero ice cover, and the relaxed bed topography, running with an ELA of 400 m a.s.l. for 15,000 years. (a) Graph of ice-sheet volume with time. Maps of ice thickness are provided at (b) 2500, (c) 5000, (d) 7500, (e) 10,000, and (f) 12,500 years of model time.

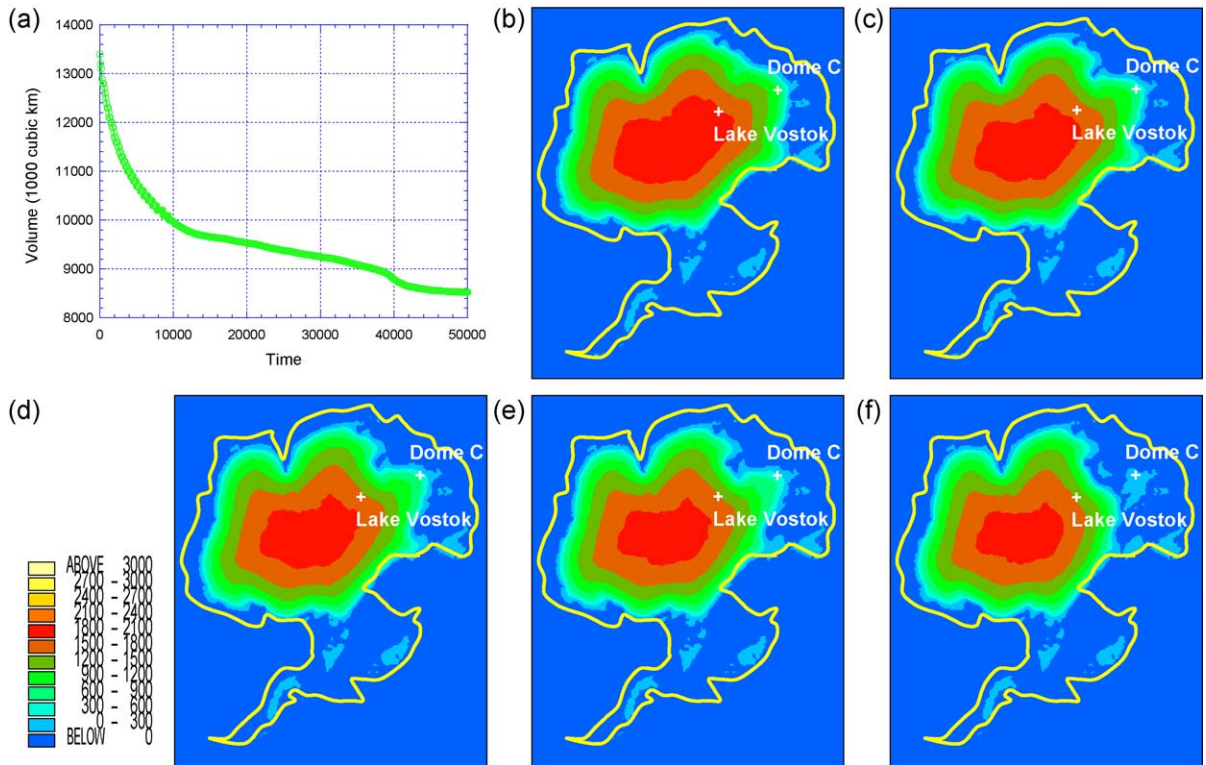


Fig. 8. Numerical ice-sheet modelling results of ice decay in East Antarctica, starting from the steady-state results shown in Fig. 7, running with an ELA of 900 m a.s.l. for 50,000 years. (a) Graph of ice-sheet volume with time. Maps of ice thickness are provided at (b) 5000, (c) 10,000, (d) 20,000, (e) 35,000, and (f) 50,000 years of model time.

flow across Dome C. The model used in this investigation is detailed in Siegert et al. (1999). Two simple experiments were performed. The first grew ice across East Antarctica, starting with zero ice cover and the isostatically relaxed bedrock. An equilibrium line altitude (ELA) of 400 m a.s.l. was emplaced across the continent, and the model run until steady state was achieved (at about 13,000 years). The second experiment started with the steady state results of the first experiment and raised the ELA to 900 m a.s.l. Steady state in this second run took around 50,000 years of model time. The results from these simple experiments are shown in Figs. 7 and 8. In the model, ice growth occurs initially from the highest elevations across, principally, the Gamburtsev Mountains (Dome A) and the area surrounding this high ground. A small ice cap forms across Dome C, which has radial flow. The centre of this ice cap is located where bed roughness is greatest in Dome

C. This style of glacial initiation was discussed by Drewry (1975) to be the origin of the macrolandscape around Dome C and has also been modelled (in a more sophisticated manner) by DeConto and Pollard (2003). As ice growth continues, the Dome C ice cap gets subsumed by a larger ice mass emanating from the Gamburtsev Mountains. By the time a steady state is achieved, the flow patterns of the ice sheet resemble that of the modern ice sheet reasonably well (i.e., no radial ice flow across Dome C). Subsequently, by raising the ELA to 900 m a.s.l., ice retreat is modelled. Ice decays from the lowest elevations around Dome C such that a radially flowing ice mass is quickly reestablished. Around 35,000 years of model time, the ice mass decays further and the ice divide retreats to the high ground west of what is now Lake Vostok.

The growth and decay of an ice sheet across Dome C is possible if the ELA varied between 400 and 900

m. Such a situation would be similar to the climate of Svalbard today. As the ice sheet grew and retreated across Dome C, the ice-sheet margin, where ice flows quickest, would have migrated across the Wilkes and Aurora basins. This glacial scenario is highly compatible with the measured smooth topography in these regions.

9. Summary and conclusions

Subglacial roughness was calculated across East Antarctica through the spectral analysis of bed measurements established from airborne RES data. Calculations were made at three intervals: high (wavelengths ~5–10 km), medium (wavelengths between 10 and 20 km), and low frequencies (wavelengths >20 km). Roughness values were compared with results from numerical ice-sheet modelling, which indicate basal thermal regime, the production of subglacial water, and the likelihood of subglacial sliding. This comparison revealed the following results concerning subglacial topography and the overlying ice sheet (Table 1).

- The morphology of subglacial Antarctica is organised into spatially coherent regions that have a characteristic roughness. We identify three main groups of subglacial roughness. Group 1 is where the bed is rough at all frequencies; Group 2 is where the bed is smooth at high frequency and rough at others; and Group 3 is where the bed is smooth at all frequencies.
 - The ice divides of Ridge B and Dome A are underlain by a bed that is rough at all frequencies analysed (i.e., Group 1). Here, the ice sheet is frozen to the bed, and it is unlikely that warm-based conditions could exist in these places while the ice sheet is in its present state.
 - At Dome C, however, the bed is rough at low and medium frequencies (i.e., subglacial valleys and hills are present) and relatively smooth at high frequency (Group 2). The ice sheet at Dome C is wet based, and there is considerable production of meltwater. However, subglacial sliding is not predicted here, and hence, it is unlikely that the present ice sheet is responsible for the smooth bed relief.
 - Where the bed is below sea level, the bed roughness is found to be generally low, especially at high frequencies (Fig. 3a).
 - Across the Wilkes and Aurora subglacial basins (Group 3), the bed is smooth at all frequencies. In these places, the ice sheet is warm based and subglacial sliding is predicted, which is compatible with the roughness calculations.
 - The Porpoise Subglacial Highlands are characterised by rough subglacial terrain at all frequencies (Group 1). The ice sheet is predicted to be cold based in this region, and, furthermore, it is difficult to envisage an ice sheet that would result in warm-based conditions in this locale.
- With the exception of the Dome C region, the bed roughness distribution appears compatible with the modern ice-sheet configuration. However, the bed at Dome C displays a morphology that is inconsistent with the present ice configuration. The following conclusions are thus drawn as explanation for the bed morphology of Dome C.
- Low-frequency subglacial troughs and valleys, if they have a glacial origin, were formed by an ice sheet whose margin was much closer to Dome C than at present and whose flow was radial about the centre of Dome C, where the bed is roughest.
 - Numerical modelling reveals that the main regions where ice decay is likely to happen are the Wilkes and Aurora subglacial basins. This leaves Dome C isolated, and radial flow across the high ground occurs. The climate required for such an ice sheet is broadly similar to that on Svalbard today.
 - As the ice sheet margin migrated across the Wilkes and Aurora basins, they would have been subject to fast-flowing eroding ice, which is compatible with the smoothed topography measured there.
- Finally, it should be noted that we have no information with regard to the timing of the ice sheet that is responsible for the morphology at Dome C. To address this issue, the modelling of ice-sheet erosion and deposition could be used to determine the timeframes required to build and maintain the subglacial morphology of East Antarctica measured in this paper.

Acknowledgements

Funding for this project was provided by NERC grants NER/A/S/2000/01256, NER/A/S/1999/00178, and the NERC Centre for Polar Observation and Modelling (CPOM). We wish to thank the reviewers of this paper, Dr. Chris Clark and Prof. Michael Hambrey, for providing valuable and insightful comments.

References

- Bamber, J.L., Baldwin, D.J., Gogineni, S.P., 2004. A new bed elevation data set for modelling the Greenland ice sheet. *Ann. Glaciol.* 37, 351–356.
- Dalziel, I.W.D., Lawver, L.A., 2001. The lithospheric setting of the West Antarctic Ice Sheet. In: Alley, R.B., Bindschadler, R.A. (Eds.), *The West Antarctic Ice Sheet: Behaviour and Environment: Antarctic Research Series*, vol. 77. American Geophysical Union, Washington, DC, pp. 29–44.
- DeConto, R.M., Pollard, D., 2003. Rapid Cenozoic glaciation of Antarctica induced by declining atmospheric CO₂. *Nature* 421, 245–249.
- Dowdeswell, J.A., Siegert, M.J., 1999. The dimensions and topographic setting of Antarctic subglacial lakes and implications for large-scale water storage beneath continental ice sheets. *Geol. Soc. Amer. Bull.* 111, 254–263.
- Drewry, D.J., 1975. Initiation and growth of the East Antarctic Ice Sheet. *J. Geol. Soc. (Lond.)* 131, 255–273.
- Drewry, D.J., 1983. *Antarctica: glaciological and geophysical folio*, Scott Polar Research Institute, University of Cambridge.
- Engelhardt, H., Kamb, B., 1997. Basal hydraulic system of a West Antarctic ice stream: constraints from borehole observations. *J. Glaciol.* 43 (144), 207–230.
- Giovinetto, M.B., Waters, N.M., Bentley, C.R., 1990. Dependence of Antarctic surface mass balance on temperature, elevation, and distance to open ocean. *J. Geophys. Res.* 95 (D4), 3517–3531.
- Hubbard, B.P., Siegert, M.J., McCarroll, D., 2000. On the roughness of glacier beds: spectral evidence of the interaction between ice flow and erosion. *J. Geophys. Res.* 105 (B9), 21295–21304.
- Huybrechts, P., 2002. Sea-level changes at the LGM from ice-dynamic reconstructions of the Greenland and Antarctic ice sheets during the glacial cycles. *Quat. Sci. Rev.* 21 (1–3), 203–231.
- Kearey, P., Brooks, M., 1991. *An Introduction to Geophysical Exploration*. Blackwell Science, 254 pp.
- Lythe, M.B., Vaughan, D.G., the BEDMAP Consortium, 2001. BEDMAP: a new ice thickness and subglacial topographic model of Antarctica. *J. Geophys. Res.* 106, 11335–11351.
- Miller, M.F., Mabin, M.C.G., 1998. Antarctic Neogene landscapes—in the refrigerator or in the deep freeze? *GSA Today* 8 (4), 1–2.
- Ó Cofaigh, C., Pudsey, C.J., Dowdeswell, J.A., Morris, P., 2002. Evolution of subglacial bedforms along a paleo-ice stream, Antarctic Peninsula continental shelf. *Geophys. Res. Lett.* 29 (8), doi:10.1029/2001GL014488.
- Payne, A.J., 1998. Dynamics of the Siple Coast ice streams, West Antarctica: results from a thermomechanical ice sheet model. *Geophys. Res. Lett.* 25, 3173–3176.
- Payne, A.J., 1999. A thermomechanical model of ice flow in West Antarctica. *Clim. Dyn.* 15, 115–125.
- Robin, G. de Q., 1969. Antarctic RES: *Philos. Trans. R. Soc. Lond.* 265A (1166), 437–505.
- Rémy, F., Tabacco, I.E., 2000. Bedrock features and ice flow near the EPICA ice core site (Dome C, Antarctica). *Geophys. Res. Lett.* 27, 405–408.
- Siegert, M.J., 2000. Radar evidence of water-saturated sediments beneath the central Antarctic ice sheet. In: Maltman, A., et al., (Eds.), *The Deformation Of Glacial Materials*. *Spec. Publ. Geol. Soc.*, 176, 217–229.
- Siegert, M.J., Dowdeswell, J.A., 1996. Spatial variations in heat at the base of the Antarctic ice sheet from analysis of the thermal regime above sub-glacial lakes. *J. Glaciol.* 42, 501–509.
- Siegert, M.J., Ridley, J.K., 1998. Determining basal ice sheet conditions at Dome C, Central East Antarctica, using satellite radar altimetry and airborne radio-echo sounding information. *J. Glaciol.* 44, 1–8.
- Siegert, M.J., Dowdeswell, J.A., Gorman, M.R., McIntyre, N.F., 1996. An inventory of Antarctic subglacial lakes. *Ant. Sci.* 8, 281–286.
- Siegert, M.J., Dowdeswell, J.A., Melles, M., 1999. Late Weichselian glaciation of the Eurasian High Arctic. *Quat. Res.* 52, 273–285.
- Siegert, M.J., Taylor, J., Payne, A.J., Hubbard, B.P., 2004. Subglacial roughness in the Siple Coast region of West Antarctica. *Earth Surf. Processes Landf.* 29, doi:10.1002/esp.1100.
- Taylor, J., Siegert, M.J., Payne, A.J. and Hubbard, B.P., 2004. Regional-scale bed roughness beneath ice masses: measurement and analysis. *Computers and Geosciences* 30, 899–908.
- Vaughan, D.G., Bamber, J.L., Giovinetto, M., Russell, J., Cooper, A.P.R., 1999. Reassessment of net surface mass balance in Antarctica. *J. Climate* 12 (4), 933–946.